Dilute Solution Routes to Various Controllable Morphologies of MCM-41 Silica with a Basic Medium†

Qiang Cai,*,‡ Zhong-Sheng Luo,‡ Wen-Qin Pang,§ Yu-Wei Fan,‡ Xi-Hua Chen,‡ and Fu-Zhai Cui‡

Department of Materials Science & Engineering, Tsinghua University, Beijing 100084, People's Republic of China, and Key Laboratory of Inorganic Synthesis & Preparative Chemistry and Department of Chemistry, Jilin University, Changchun 130023, People's Republic of China

Received October 19, 1999. Revised Manuscript Received June 2, 2000

MCM-41 silica particles with several morphologies have been controllably synthesized with a basic medium. Nanospherical MCM-41 silica with an average size of 110 nm was produced through reaction of extremely low surfactant concentrations of CTAB with TEOS in the sodium hydroxide medium at 353 K, while a submicrometer-sized silica rod, 0.3−0.6 μm in diameter and 1 μm in length, and micrometer-sized oblate silica with nominal diameter around 1 μm were synthesized in aqueous ammonia, where the size and the morphology were controlled by varing the content of the solvent. A morphogenetic mechanism that is based on the deposition of self-assembled silicate surfactant rodlike micelles is proposed and explains well the controllability of the morphology.

I. Introduction

The synthesis of mesoporous materials with structures over length scales from nanometer to micrometer has ramifications in diverse areas, such as catalysis,[1] biomolecule separations, chromatographic supports, development of medical implants, miniaturization of electronic devices, and formation of semiconductor nanostructures.[2] Specially, the synthesis of beads of defined size could open up new possibilities for application of MCM-41 as a packing material in chromatography or as an easy-to-handle form of MCM-41 for catalytic purposes.

Research in the preparation of materials that contain both surfactant-templated mesoporosity and controlled bulk features has just begun.[3] Ozin and co-workers[4] first demonstrated the co-presence of various morphologies of mesoporous silicates particles under acidic conditions. The materials were synthesized in an extremely dilute solution of TEOS and surfactant with very low pH conditions. Huo et al.[5] demonstrated that mesoporous silica could be produced in the form of marblelike spheres of about 1 mm in diameter. The size of the spheres was reported to be controlled by the stirring speed. Grün et. al.[6] reported the synthesis of spherical silica particles featuring the MCM-41 structure, whose size ranged from 400 to 1100 nm. Their synthesis procedure was a modification to Stöber's synthesis[7] of monodisperse silica spheres by adding cationic surfactant to the reaction mixture during the formation of MCM-41. Recently, Büchel et al.[8] reported a novel method for the synthesis of submicrometer-sized (≈700 nm) solid core/mesoporous shell silica spheres. Their method was based on a combination of the Stöber approach,[8] the Unger growth process,[9] and the Kaiser approach.[10]

Although various morphologies have been previously achieved, little is known about the formation and control of the morphologies of MCM-41. In the present paper, we report the control of morphologies of silica particles, where nanospheres, submicrometer-sized rods, and micrometer-sized oblate particles of MCM-41 silica are produced. A formation mechanism was proposed to interpret the morphogenetic control on the basis of deposition of self-assembled silicate rodlike micelles.

II. Experimental Section

Chemical Agent. In this study, hexadecyltrimethylammonium bromide (CTAB) was used as the cationic surfactant, while tetraethyl orthosilicate (TEOS) served as the silica

* To whom correspondence should be addressed.

† This work was supported by the National Natural Science Foundation of China.

‡ Tsinghua University.

§ Jilin University.

(1) Hoppe, R.; Ortlam, A.; Rathousky, J.; Schulz, G.; Zukel, E. A. *Microporous Mater.* **1997**, *8*, 267.

(2) Chomski, D., O.; Kuperman, A.; Coombs, N.; Ozin, G. A. *Chem. Vap. Deposition* **1996**, *2* (1), 8−13.

(3) (a) Oliver, S.; Kuperman, A.; Coombs, N.; Lough, A.; Ozin, G. A. *Nature* **1995**, *378*, 47. (b) Davis, S. A.; Burkett, S. L.; Mendelson, N. H.; Mann, S. *Nature* **1997**, *385*, 420. (c) Schacht, S.; Huo, Q.; Voigt-Martin, I. G.; Stucky, G. D.; Schüth, F. *Science* **1996**, *273*, 768.

(4) (a) Yang, H.; Coombs, N.; Sokolov, I.; Ozin, G. A. *J. Mater. Chem.* **1997**, *7*, 1285. (b) Yang, H.; Coombs, N.; Ozin, G. A. *Nature* **1997**, *386*, 692. (c) Oliver, S.; Kuperman, A.; Coombs, N.; Lough, A.; Ozin, G. A. *Nature* **1995**, *378*, 47.

(5) Huo, Q.; Zhao, D.; Feng, J. L.; Weston, K.; Buratto, S.; Stucky, G. D.; Schacht, S.; Schuth, F. *Adv. Mater.* **1997**.

(6) Grün, M.; Lauer, I.; Unger, K. K. *Adv. Mater.* **1997**, *9* (3), 254.

(7) Stöber, W.; Fink, A.; Bohn, E. *J. Colloid Interface Sci.* **1968**, *26*, 62.

(8) Büchel, G.; Unger, K. K.; Matsumoto, A.; Tsutsumi, K. *Adv. Mater.* **1998**, *10* (13), 1036.

(9) Unger, K. K.; Giesche, H.; Kinkel, J. N. German Patent DE-3534 143.2, 1985.

(10) Kaiser, C.; Unger, K. K. German Patent DE-195 30031 A1, 1997.

10.1021/cm990661z CCC: $20.00
Published on Web 01/06/2001

Table 1. Synthesis Conditions of the MCM-41 Silica Particles and Starting Materials Composition[a]

no.	composition	product
sample 1	1197(H_2O) 0.31(NaOH) 0.125(CTAB) 1(TEOS)	nanometer MCM-41 sphere
sample 2	525(H_2O)69(NH_4OH)0.125(CTAB)1(TEOS)	micrometer MCM-41 sphere (concluding hexagonal crystal)
sample 3	1050(H_2O)138(NH_4OH)0.125(CTAB)1(TEOS)	micrometer MCM-41 rod
sample 4	525(H_2O)69(NH_4OH)0.125(CTAB)0.16(TEOS)	urchin-like agglomerates

[a] Reaction temperature: RT. Reaction time: 2.0 h.

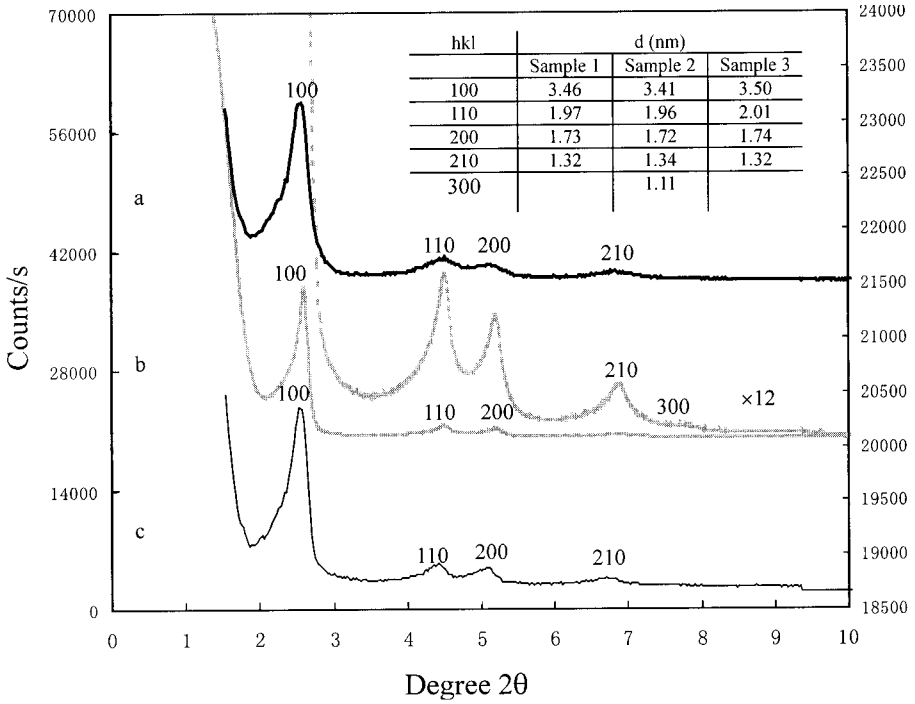

Figure 1. X-ray diffraction pattern of MCM-41 samples obtained after calcination at 823 K of (a) sample 1, (b) sample 2, and (c) sample 3.

source. Aqueous sodium hydroxide or ammonia was used as the catalyst. CTAB, ammonia, and sodium of A. R. were purchased from Beijing Xizhong Chemical Plant. TEOS of A. R. was obtained from Shenyang Chemical Agent Plant I. The distilled water with the electrical conductivity that is larger than 7 MΩ was used as the solvent.

Procedure. Typical syntheses of ordered MCM-41 silica particles were introduced to illustrate the situation of controlling the size of the particles. Four routes were opted to synthesize the MCM-41 silica particles as shown in Table 1. The synthetic conditions are both strong stirring with an extremely low surfactant concentration at 353 K. Typically, the synthesis procedures of sample 1 were as follows: (1) 3.5 mL of NaOH (2 M) solution was mixed with 480 mL of distilled water; (2) 1.0 g of surfactant was added to the solution with stirring and heating; (3) when the solution became homogeneous, 5 mL of TEOS was dropped in slowly, giving rise to a white slurry; (4) after 2 h, the resulting product was filtered, washed with distilled water, dried at ambient temperature, and followed by calcination in air at 823 K for 4 h.

Characterization. To investigate the structure and crystallinity of the samples, the powders were analyzed with an X-ray powder diffractometer, XRD (D/max-rA Rigaku diffractometer, Cu Kα radiation (λ = 1.5418 Å), Japan). The sample was scanned from 0.8° to 10° (2θ) with a step size of 0.02° and a count time of 1 s at each point.

Adsorption and desorption isotherms for nitrogen were obtained at 77 K using a Micromeritics ASAP-2010. The samples were outgassed at 573 K for 12 h before measurements were performed. Specific surface area values were obtained using the BET (Brunauer−Emmett−Teller) equation.

Sample morphology and microstructure were examined by scanning electron microscopy, SEM (HITACHI X-650 scanned electron microscope, Japan), and by transmission electron microscopy, TEM (Hitachi-8100 transmission electron microscope (operated by 200KV), Japan). For TEM analysis, specimens were prepared by dispersing the as-obtained powder in alcohol and then placing a drop of the suspension on a copper grid coated with a transparent graphite, followed by drying.

III. Results and Discussion

Results. The diffractograms of the materials studied are shown in Figure 1. Sample 1 (catalyst: NaOH, H_2O/TEOS = 1197) exhibits four sharp Bragg peaks, which can be indexed as (100), (110), (200), and (210) of MCM-41 (Figure 1a). The repeat distance, a_0, between two pore centers in MCM-41 can be calculated from

$$a_0 = (2/\sqrt{3})d_{100} \quad (1)$$

The pore diameter can therefore be calculated from a_0 by subtraction of 1.0 nm, which is an approximated value of the pore wall thickness.[11] Using the d_{100} value of 3.463 nm, the pore diameter of 3.00 nm is finally obtained. The diffractogram of sample 2 (catalyst: NH_4-OH, H_2O/TEOS = 525) shows five distinguishable peaks including a strong peak around 2.55° and four weak peaks at 4.41°, 5.09°, 5.89°, and 6.70°, which correspond to (100), (110), (200), (210), and (300) of MCM-41,

(11) Chen, C. Y.; Burkett, S. L.; Li, H. X.; Davis, M. E. *Microporous Mater.* **1993**, *2*, 27−34.

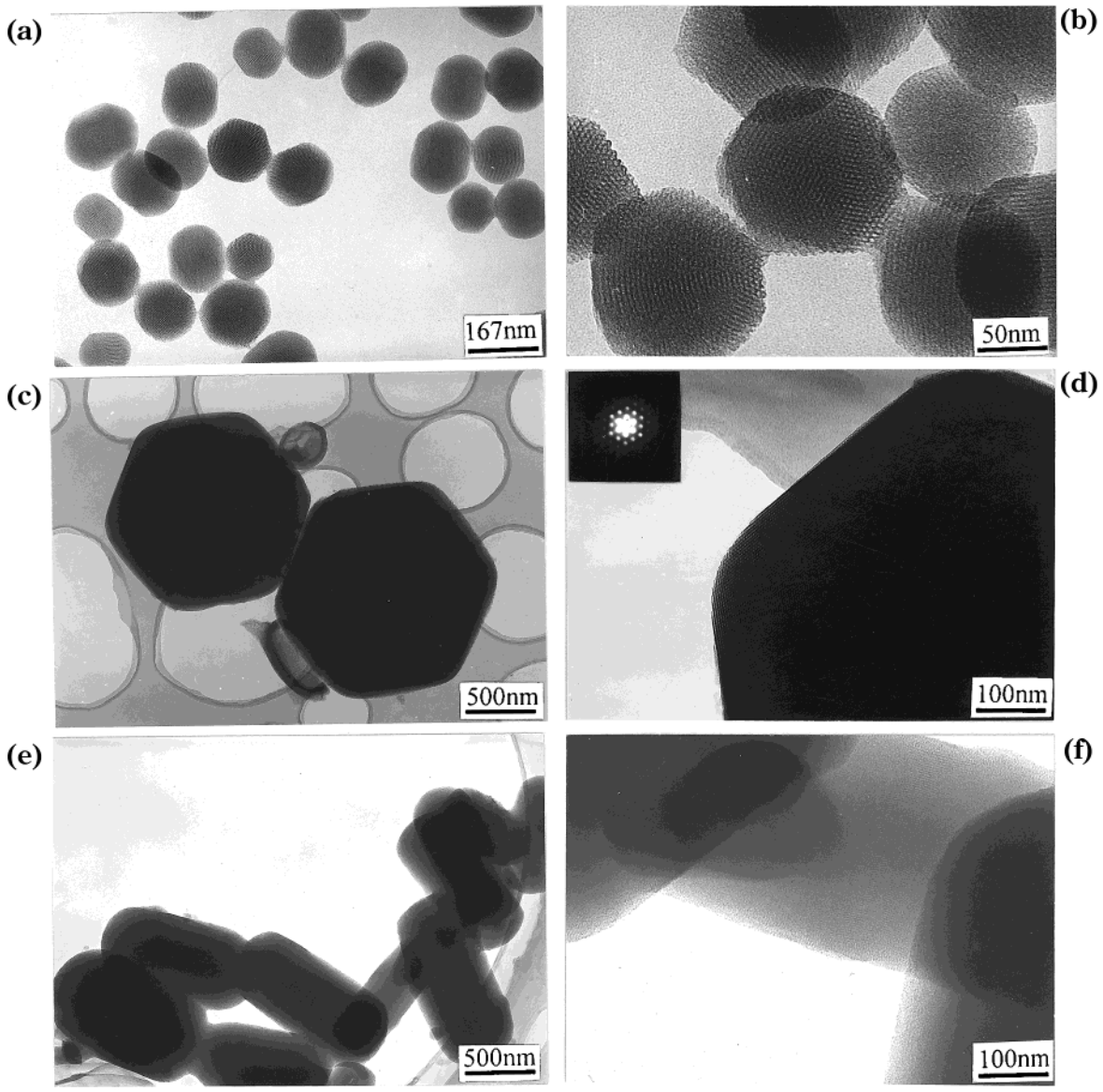

Figure 2. TEM image of the calcined materials: (a) sample 1 (scale bar, 167 nm); (b) sample 1 (scale bar, 50 nm); (c) sample 2 (scale bar, 500 nm); (d) sample 2 (scale bar, 100 nm); (e) sample 3 (scale bar, 500 nm); (f) sample 3 (scale bar, 100 nm).

respectively, suggesting perfect long-range order in this material (Figure 1b). Calculation of the pore diameter gives a value of 3.01 nm. The diffractogram of sample 3 (catalyst: NH_4OH, H_2O/TEOS = 1055) also shows five distinguishable peaks that are similar to those of samples 1 and 2, suggesting perfect long-range order in this material (Figure 1c).

The morphologies and microstructure of the obtained MCM-41 samples are clearly revealed by TEM. Figure 2a shows the typical TEM images of sample 1, where nanosized particles of near sphere or elongated sphere can be consistently seen. The sizes of the particles range from 60 to 140 nm. HRTEM images of the sample (Figure 2b, scale bar, 50 nm) show the existence of highly ordered hexagonal array and streak structural features. The hexagonal array is the view of the crystals whose *c* axis parallels the line of vision, and the streak is that of the crystals whose *c* axis is perpendicular to the line of vision. Figure 2c,d shows the representative TEM image of sample 2. Perfect hexagonal single crystals of MCM-41 without intergrowth and twinned aggregation are clearly evident in the figure (Figure 2c). Enlargement of the crystals (Figure 2d) further show that they are structured with a long-range highly ordered hexagonal array of pores. Their macroscopic hexagonal feature is very consistent with their mesoscopic hexagonal structural units, indicating that the mesoporous mateirlas here might be obtained by the stacking of silicate micelles instead of the phase transformation of sol−gel. Figure 2e shows the representative TEM image (scale bar, 500 nm) of sample 3. It can be seen that the obtained MCM-41 is rodlike featured, with 0.7−1 μm in length, 0.3−0.5 μm in width, and aspect ratios (length/width) of about 2−3. HRTEM (Figure 2f) images further reveal that the *c* axis of the obtained MCM-41 parallels the axis of the rod.

Although the nitrogen adsorption and desorption properties of micrometer-sized particles of MCM-41 have been well documented,[7] such properties of nanosized particles of MCM-41 have not been reported before and are therefore unknown up to this date. In the present paper we for the first time investigate nitrogen adsorption and desorption properties of MCM-41 particles with sizes of around 100 nm. To reveal the special

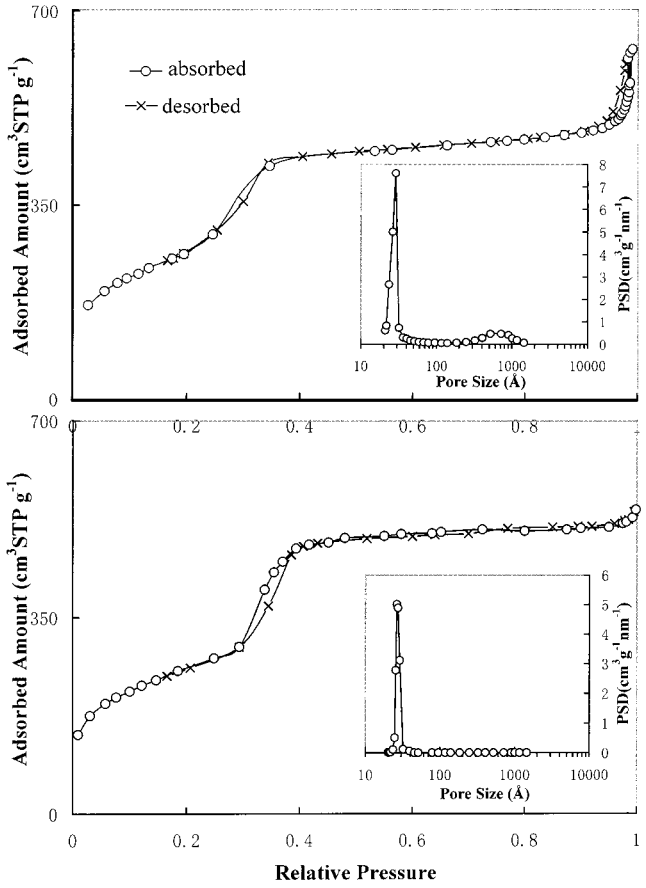

Figure 3. Nitrogen sorption isotherms obtained at 77 K and pore size distributions of (a) sample 1 and (b) sample 2.

character of the nanosized particles of MCM-41, we use micrometer-sized particles of MCM-41 as the control. As a typical example, we choose sample 2 as the control. Nitrogen isotherms of samples 1 and 2 are shown in Figure 3a, b, where the isotherms can be classified as type IV isotherms according to the IUPAC nomenclature.[12] Similar phenomena were observed in both samples. A linear increase of absorbed volume at low pressures is followed by a steep increase in nitrogen uptake at a relative pressure of $0.24 < p/p_0 < 0.34$ for sample 1 and $0.30 < p/p_0 < 0.40$ for sample 2, respectively, which is due to capillary condensation inside the mesopores. The long plateau at higher relative pressures indicates that pore filling is restricted to the inflection point at $p/p_0 = 0.30$ for sample 1 and 0.35 for sample 2, respectively. An obvious difference between the isotherms is that another steep increase occurs in nitrogen uptake and an adsorbed hysteresis loop appears at a relative pressure $0.9 < p/p_0 < 1.0$ for sample 1 while no such phenomenon occurs for sample 2. The Barret−Joyner−Halenda (BJH) method was applied to calculate the pore size distribution. The results further indicate that sample 1 (insert) possesses both pores, averaging 3 nm in diameter with narrow pore size distributions and pores averaging 70 nm in diameter with relative broad pore size distributions, while sample 2 possesses only pores averaging 2.9 nm in diameter which is very consistent with that of the published literature.[13] A summary of all parameters obtained by nitrogen sorption and XRD is shown in Table 2.

Table 2. Material Properties of MCM-41[a]

	catalyst	specific surface area (m^2/g)	specific pore volume (cm^3/g)	average pore diameter (XRD) (nm)	average pore diameter (N_2 sorption) (nm)
sample 1	NaOH	965	0.84	3.00	3.49 (3.04,[b] 70[c])
sample 2	NH_4OH	1020	0.93	2.94	2.90

[a] Specific surface area: BET equation; pore diameter (XRD): $d_{100} \times 2/\sqrt{3} - 1.0$ nm (pore wall thickness); specific pore volume: single-point volume at $p/p_0 = 0.98$; average pore diameter (N_2 sorption): $4V_p/a$, by BET. [b] Pore size at maximum of pore volume in the mesopore range. [c] Pore size maximum of pore volume in the macropore range.

Detailed investigation of sample 1 shows that macropores revealed by the pore size distribution curve of sample 1 correspond to interstices among nanometer spheres. SEM images of the sample directly illustrate the conclusion. Figure 4a shows the SEM image of sample 1 where small spherical particles of mesoporous silica MCM-41 with diameters of 90−160 nm are evident. It can be clearly seen that the nanoparticles stack compactly and particle interstices with nominal diameter averaging 100 nm are consistently found. Figure 4b shows the SEM image of sample 2. Larger particles of mesoporous silica MCM-41 ranging from 500 to 3000 nm with an average size of 1000 nm exist here and a looser packing of the particles is observed. The interstices are too large in size to be detected; that is why they cannot be seen in the pore size distribution curve of sample 2.

Mechanism of the Morphology Formation. We propose that the morphology control is achieved through deposition of self-assembled rodlike silicate micelles. The morphogenesis mechanism is shematically illustrated in Scheme 1. The formation of the mesoporous silica particle begins with nucleation involving silica−surfactant interactions that facilitate the assembly of rodlike silicate micelles. First, immediately after the two precursors (surfactant and inorganic solution containing predominantly multiply charged silicate anions at a certain pH) are mixed, ion exchange of silicate oligomers with Br^- and OH^- anions occurs to form inorganic−organic self-assembled silicate micelles (SSMs), which might not be formed at the sufactant conditions used without the presence of a silicate oligomer. To verify the presence of SSM, the experiment with the low concentration of TEOS ($^1/_6$ the concentration of TEOS of sample 2) were carried out, whose detailed synthesis condition is specified as sample 4 in Table 1. A typical morphology of the sample is given in Figure 5, where urchin-like agglomerates are consistently evident. We propose that the agglomerates are formed by the random deposition of the SSM. Second, the length of silicate rodlike micelles are determined according to the catalyst of NaOH or NH_4OH, that is, the NH_4OH medium favors

(12) IUPAC, Reporting Physisorption Data for Gas/Solid Systems. *Pure Appl. Chem*. **1957**, *87*, 603.

(13) (a) Kresge, C. T.; Leonowicz, M. E.; Roth, W. J.; Vartuli, J. C.; Beck, J. S. *Nature* **1992**, *359*, 710. (b) Beck, J. S.; Vartuli, J. C.; Roch, W. J.; Leonowicz, M. E.; Kresge, C. T.; Schmitt, K. D.; Chu, C. T.-W.; Olson, D. H.; Sheppard, E. W.; McCulen, S. B.; Higgins, J. B.; Dchlenker, J. L. *J. Am. Chem. Soc.* **1992**, *114*, 10834.

(14) Firouzi, A.; Kumar, D.; Bull, L. M.; Besier, T.; Siegev, P.; Huo, Q. S.; Walker, S. A.; Zasadzinski, J. A.; Glinka, C.; Nicol, J.; Margolese, D. A.; Stucky, G. D.; Chmelka, B. F. *Science* **1995**, *267*, 1138.

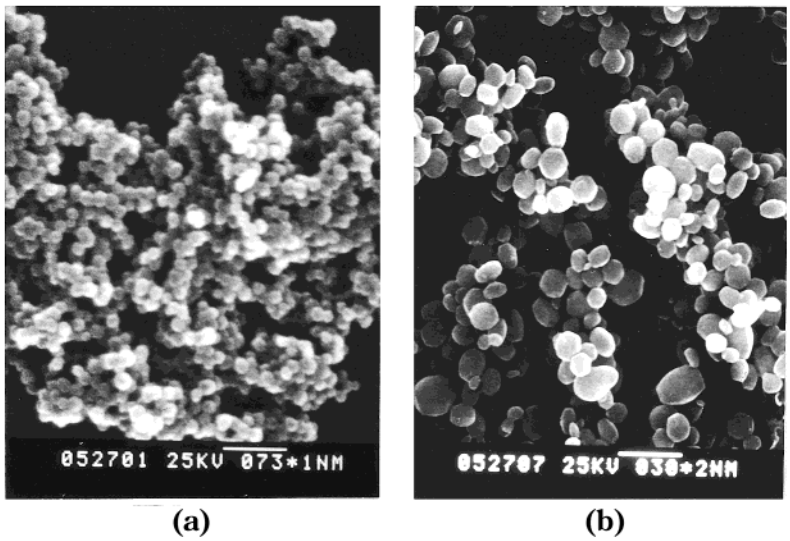

Figure 4. SEM micrographs of calcined materials: (a) sample 1 (scale bar, 720 nm); (b) sample 2 (scale bar, 3000 nm).

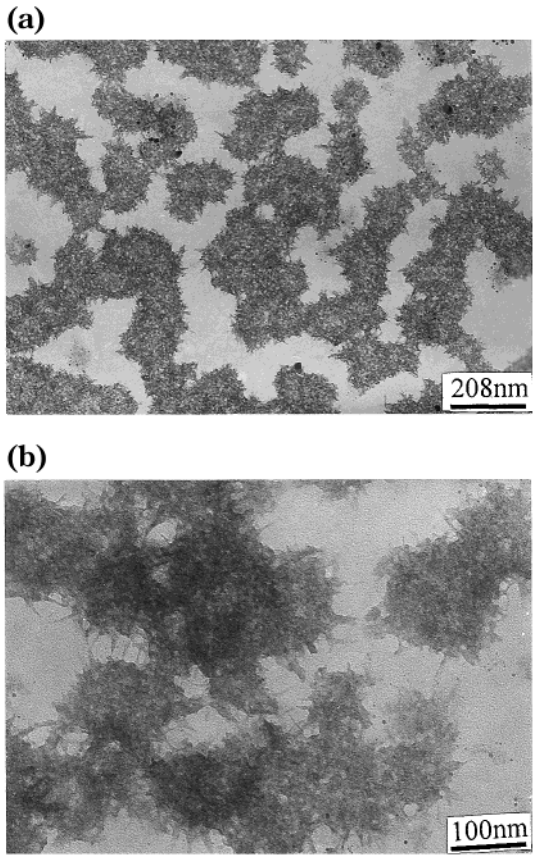

Figure 5. TEM image of the as-synthesized sample 4: (a) scale bar, 208 nm; (b) scale bar: 100 nm.

longer micelles and NaOH shorter micelles. It is well-known that the ratio of the interaction of the silicate oligomers among the Gouy−Chapman region to that of the hydrocarbon chains resulting from the van der Waals forces is related to the curvature of the formed micelles.[15] Because the combination of silicate oligomers among the Gouy−Chapman region in the NH_4OH medium is stronger than that in NaOH, longer micelles are favored in the NH_4OH medium, which is consistent with our observations. Finally, the electrostatic interactions among and the condensation of the rodlike silicate micelles facilitate the deposition of the micelles. As a result, mesoporous silica with various morphologies are formed: in the dilute solution of NaOH, short SSMs lead to the formation of a nanosphere of MCM-41; while in the NH_4OH medium, longer SSMs assemble into urchin-like agglomerates, submicrometer-sized silica rods, and micrometer-sized oblate silica in terms of the concentration of TEOS or CTAB. Urchin-like agglomerates are formed because of a limited source of silicate oligomers where the concentration of TEOS is much lower than that of other samples. And the low concentration of CTAB results in a low concentration of SSM, leading to the formation of rodlike submicrometer MCM-41. With a slightly high concentration of CTAB, the concentration of the SSM increases consequently, favoring the formation of MCM-41 particles with a larger size. Notably, high regularity of the shape of the obtained particles of MCM-41 (Figure 6) and the high-order structure of the particles (Figure 2) further point out that the particles are formed by the deposition of the SSM rather than one-step self-assembly of the silicates and surfactants. Figure 6 shows the representative SEM images of the single crystal of MCM-41 (sample 2). A single crystal of MCM-41 in the shape of a hexagon can grow to be as large as 4×4 μm (arrow in Figure 6b). Enlargement of one of the single crystals (Figure 6a) clearly shows that the hexagonal MCM-41 particles are highly regular in shape.

IV. Conclusions

In summary, a new route for control of mesoporous silica with various morphologies on the nanometer and micrometer scale was introduced. Despite varying concentrations of CTAB, TEOS, and changing catalyst, nanospheres of MCM-41 silica with an average size of 100 nm, submicrometer-sized MCM-41 rods with 0.7−1 μm in length, 0.3−0.5 μm in width, and aspect ratios (length/width) of about 2−3, and micrometer-sized oblated silica ranging from 500 to 2500 nm with an average size of 1000 nm have been controllably synthesized. Especially the nanosphere of MCM-41 exhibits unusual hierachical pore structure, which correspond

(15) Patterson, L. K.; Vieil, E. *J. Phys. Chem.* **1973**, *77*, 1191.

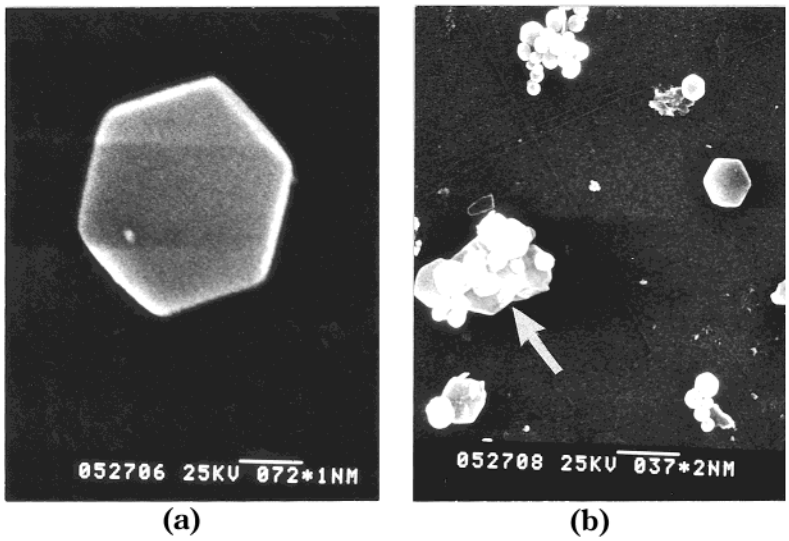

Figure 6. SEM micrographs of calcined materials: (a) sample 2 (scale bar, 3700 nm); (b) sample 2 (scale bar, 720 nm).

Scheme 1

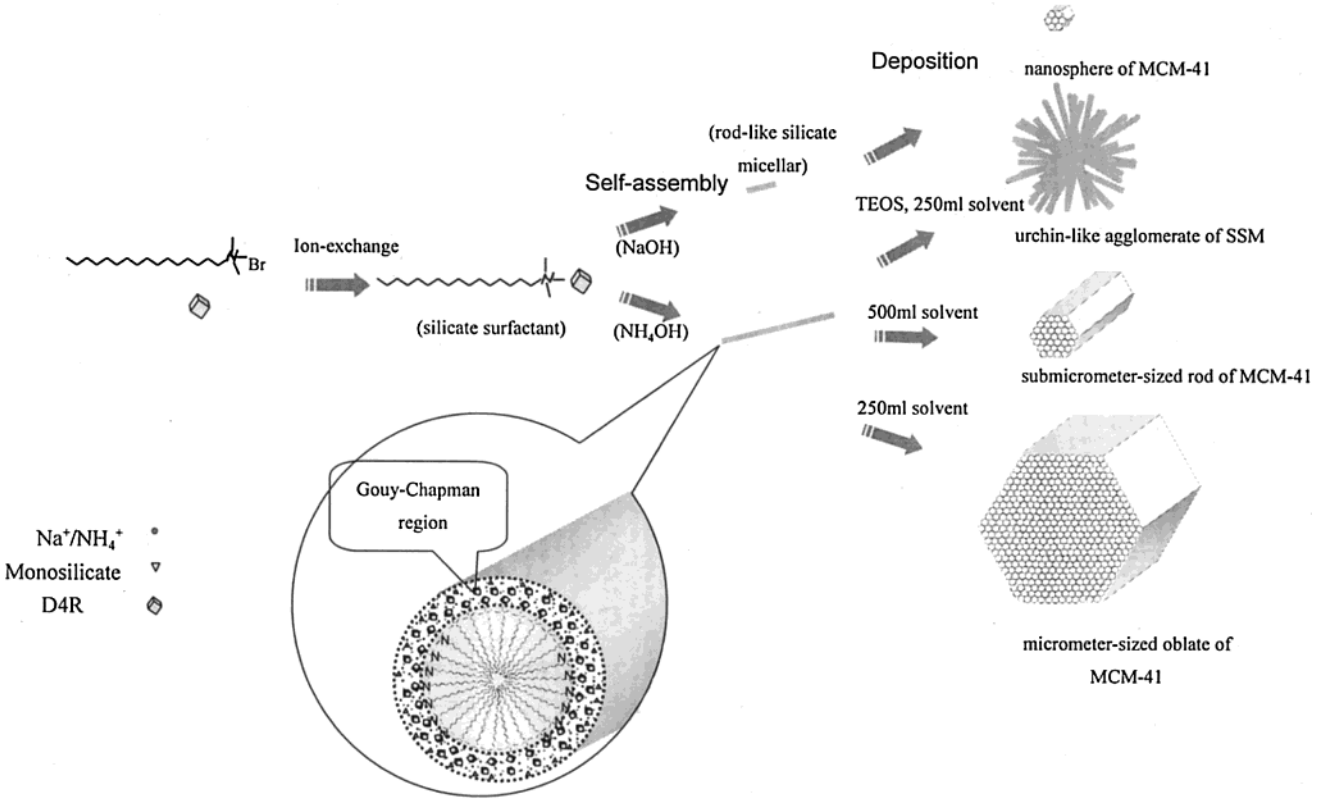

to surfactant-templated mesoporosity (3 nm) and interstices among nanometer spheres (≈70 nm). Such pore structure and its thermal stability make the nanometer-size MCM-41 silica suitable as adsorbents for capillary electro-endosmotic chromatography (CEC). Furthermore, the experimental results suggest that the growth of the MCM-41 particles and their morphology control are accomplished through a deposition process of self-assembled silicate micelles (SSM). The present method and proposed mechanism are helpful in designing and preparing large mesoporous single crystals, which can greatly improve operability of mesoporous materials and make them ideal hosts for encapsulating semiconductor guests for formation of novel nanostructures and miniaturization of electronic devices.

Acknowledgment. The authors greatly thank Professor Zhonghua Jiang (Institute of Radiation Medicine Academy of Military Medical Sciences, Beijing, 100850, P. R. China) for helpful discussions.

CM990661Z